PII: S0955-2219(98)00115-0

0955-2219/98/$—see front matter

From Long-Range Interaction to Solid-Body Contact Between Colloidal Surfaces During Forming

Chu-Wan Hong*

University of Erlangen-Nürnberg, Institute of Materials Science (3), D-91058 Erlangen, Germany

(Received 18 April 1997; revised version received 16 March 1998; accepted 9 April 1998)

Abstract

A simulation method based on the discrete element method (DEM) has been developed for studying the particle packing dynamics and for optimizing the colloidal forming processes. The DEM needs explicit functions for the computation. The explicit van der Waals interaction functions derived by Hamaker between two surfaces (or spheres) become infinite if the surface distance approach zero. This is a numerical singularity problem due to the continuum assumption in the Hamaker theory and is inconsistent with the physical reality. The analytical solutions obtained by using the modern Lifshitz's theory and solution by incorporating the non-continuum theories (e.g. Lennard–Jones potential) are too complex to be applied for the DEM process simulation. During consolidation processes, the colloids move from the long-range interaction region into the solid-body contact with other colloids or with the boundaries. The long-range interaction were described by the DLVO theory. Meanwhile, the Johnson–Kendall–Roberts (JKR) theory took the adhesion energy (or surface energy) into account for describing the elastic solid-body contact. Both the Derjaguin approximation and the JKR theory based on the continuum assumption have been successfully applied to solve the transition (or numerical singularity) problem from the DLVO long-range interaction to the elastic JKR solid-body contact for the DEM simulation. Solving the transition/singularity problem is the first step for simulating the consolidation processes. In this numerical model, the adhesion energy, the elastic deformation, the hard sphere diameter and the compact Stern layer were considered. The shortest surface distance (without external load) is calculated at a distance where the JKR adhesion force is equal to the DLVO interaction force. The interactions between two spheres, between sphere and surface plane and between two different materials were shown. The DEM simulation results show that the particle-pile-up is an essential mechanism for the particles to get into solid-body contact in stabilized suspensions.

1 Introduction

Powder agglomeration has been recognized as the major factor limiting the strength and Weibull modulus of ceramics made by sintering. Ceramic green bodies fabricated by colloidal processing techniques achieve better mechanical properties[1] because the agglomeration process in suspension can be prevented by suitable stabilization. Ceramic particles are subjected to many varying interactions resulting from changing surroundings during colloidal forming process. These interactions, like particle–particle and particle–boundary interactions, frictional drag, gravitation force, hydrostatic lift, hydrodynamic lift, rotational resistance, etc., have been taken into account for the numerical simulation based on the discrete element method (DEM).[2] In the stabilized suspensions, the colloids disperse homogeneously in the solution because of their electrostatic double-layer repulsions. These colloids will approach each other and form the sediment in a forming process. This means that the colloids will move from the long-range interaction region into the solid-body contact with other colloids or with the boundaries. Therefore, both long-range interactions and particle contact have to be considered for simulating the colloidal forming processes.

*Fax: +49 9131 858311; e-mail: hong@ww.uni-erlangen.de

According to the DLVO theory, the long-range interactions include the van der Waals attraction and the electrostatic double-layer repulsion and the total interaction energy V_{tot} between any two colloidal surfaces is controlled by the van der Waals energy V_{vdw} and by the electrostatic repulsive energy V_{el},[3–5] i.e.

$$V_{tot} = V_{vdw} + V_{el}. \quad (1)$$

And the DLVO potential interaction force F_p. can be derived through differentiation of the potential interaction energy

$$\vec{F}_p = -\frac{\partial V_{tot}}{\partial h} = \vec{F}_{vdw} + \vec{F}_{el}, \quad (2)$$

where h is the surface distance.

Numerical simulation based on the DEM needs explicit functions for the computation. The van der Waals and electrostatic double layer interaction functions derived from the Hamaker theory and from the electrostatic Poisson–Boltzmann equation (see Section 2), respectively, have been successfully implemented into the DEM simulation program and have been used to study the particle packing behavior during colloidal forming processes.[6–8]

However, the DLVO theory has a restriction. It cannot describe correctly the interactions between colloidal surfaces at a very short distance (generally if $h < 5$ nm), if short-range interactions, e.g. hydration, steric interaction etc., exist.[9,10] Even for the case that only the long-range interactions exist, the explicit van der Waals interaction functions, according to the Hamaker theory, show numerical singularity when $h \to 0$ [see eqns (3) and (4)]. This is due to the poor continuum assumption of the constituent molecules as point particles and the application of the method of pairwise summation of interaction in the Hamaker theory.[11,12] Furthermore, the explicit V_{vdw} interaction functions, according to the modern dispersion theory of Liftshitz, need much mathematical effort to be solved[11] and show also divergence between two dielectric surfaces at zero separation.[12] Under consideration of the effect of the finite size of the constituent molecules on the dielectric response of the system, the divergence difficulties of Lifshitz's theory at small distances can be removed. Nevertheless, the mathematical complexity remains tremendous and is not practicable for the DEM simulation. Another solution by incorporating the non-continuum theories, e.g. Lennard–Jones molecular potential interaction, brings the simulation into a more complex level of the molecular dynamics. This will make the process simulation impossible for the applications. Furthermore, the parameters for the calculation of the molecular or atomic interaction in an aqueous solution are unknown. Meanwhile they are difficult to determine. Consequently, the singularity problem of the explicit functions derived from Hamaker theory has to be numerically solved by using the continuum assumptions, before the DEM method can be used for simulating the long-range interactions.

While the applied van der Waals interaction functions or forces become infinite if $h \to 0$ [see eqns (3) and (4)], the electrostatic repulsion will reach a finite value [see eqns (5) and (6)]. This is inconsistent with the physical reality. If no external forces act on the system, the particles pair would come into the primary energy minimum under the van der Waals attraction, but could not get closer to each other. This primary energy minimum corresponds to a shortest reachable surface distance which is controlled by the surface morphology and the atomic short-range repulsion.[3,17] The long-range interaction can be described by the DLVO theory. Independent of the DLVO theory, the Johnson–Kendall–Roberts (JKR) theory takes the adhesion energy (or surface energy) into account for describing the elastic solid-body contact.[17–20]

The DLVO theory and the JKR theory are two different theories. So far as known, no physical connections between them were formulated for solving the transition problem from the DLVO long-range interaction to the JKR solid-body contact. In this work, the transition problem will be modeled and the physical connections between them will be mathematically formulated. The derived mathematical formulations for solving the transition problem offer at the same time a physically meaningful solution for the numerical singularity problem by using the explicit van der Waals attraction functions based on the Hamaker theory. They are also the fundamentals for simulating the consolidation processes by using the DEM. This paper emphasizes the mathematical modelling and its numerical realization of the singularity problem by using the explicit interaction functions. As example, the interaction transition phenomena during the centrifuging processes of ZrO_2/Al_2O_3 suspensions were simulated and shown in this paper.

2 Explicit Long-Range Potential Interaction Functions

The van der Waals interaction energy V_{vdw} between two spheres with radii r_1, and r_2 at surface distances of h has been derived by Hamaker and has the following form:[4,5,11]

$$V_{\text{vdw}} = -\frac{A_{\text{H}}}{6}\left[\frac{2r_1r_2}{h^2+2h(r_1+r_2)} + \frac{2r_1r_2}{h^2+2h(r_1+r_2)+4r_1r_2} + \ln\left(\frac{h^2+2h(r_1+r_2)}{h^2+2h(r_1+r_2)+4r_1r_2}\right)\right] \quad (3)$$

where A_{H} is the Hamaker constant. The case of a sphere of radius r at distance h from a planar half-space (or plane) is obtained from eqn (3) by setting $r_1 = r$ and taking the limit as $r_2 \to \infty$. We obtain:

$$V_{\text{vdw}} = -\frac{A_H^r}{6h}\left[1 + \frac{h}{2r+h} + \frac{h}{r}\ln\left(\frac{h}{2r+h}\right)\right] \quad (4)$$

According to the Gouy–Chapmann model of diffuse layer and under the application of the electrostatic Poisson–Boltzmann equation, the interaction energy V_{el} between two spheres with radii r_1 and r_2 and Zeta potentials $\psi_{d1}(=\zeta_1)$ and $\psi_{d2}(=\zeta_2)$ at surface distances of h is given by the following equation:[4,5,13,14]

$$V_{\text{el}} = 64\pi\varepsilon_r\varepsilon_{\text{o}}\left(\frac{RT}{zF}\right)^2\frac{r_1r_2}{r_1+r_2} \cdot \left[\tanh\left(\frac{zF\psi_{d1}}{4RT}\right)\tanh\left(\frac{zF\psi_{d2}}{4RT}\right)\right]e^{-\kappa h}, \quad (5)$$

with

$$\kappa = \sqrt{\frac{\Sigma_i z_i^2 c_i F^2}{\varepsilon_r\varepsilon_{\text{o}}RT}}. \quad (6)$$

Here

A_{H}	is the Hamaker constant;
κ	is the Debye–Hückel parameter;
RT	is the thermal energy;
F	is the Faraday constant;
z	is the valency of the electrolyte;
c	is the concentration of electrolyte in moles;
ε_{r}	is the relative dielectric constant of the medium;
and ε_{o}	is the permittivity of free space.

For sphere and planar geometry, Ives and Gregory[15,16] give the expression:

$$V_{\text{el}} = 9{\cdot}24\times10^{-11}\tanh\left(\frac{zF\psi_{d1}}{4RT}\right)\tanh\left(\frac{zF\psi_{d2}}{4RT}\right) \cdot r\ln\left(1+e^{-\kappa h}\right). \quad (7)$$

The pair equations, eqns (3) and (5) or eqns (4) and (7), build up the total DLVO long-range interaction potentials between spheres and between sphere and plane and have been implemented into the DEM simulation program for analyzing stability of colloidal suspensions. They show a numerical singularity at zero separation (or solid-body contact), which will be numerically solved by using the following JKR theory and Derjaguin approximation.

3 Adhesion and Elastic Solid-Body Contact

For most ceramic powders with particle sizes of $d < 1\ \mu$m, the adhesion effects resulted from their high active surfaces have to be considered in the powder processing and have to be taken into account in the modelling. Modern theories of the adhesion mechanics of two elastic contacting surfaces are based on the JKR theory.[9,17] In the JKR theory, two spheres will flatten when in contact (see Fig. 1). The contact area will increase under an external load or force F. However, a finite contact area remains even if the external force disappears. Consequently, a *pull-off* force will be needed for separating two particles in contact. With the radii r_1, and r_2, Poisson's ratios ν_1, and ν_2, Young's moduli E_1 and E_2, elastic constants

$$k_{\text{el}} = \frac{1-\nu_1^2}{\pi E_1} \quad \text{and} \quad k_{e2} = \frac{1-\nu_2^2}{\pi E_2},$$
$$r^* = \frac{r_1r_2}{r_1+r_2}, \quad k_e^* = \frac{4}{3\pi(k_{e1}+k_{e2})}$$

and the adhesion work W_{ad}, the contact radius a at mechanical equilibrium is given by

$$a^3 = \frac{r^*}{k_e^*}\left[F + 3\pi r^* W_{\text{ad}} + \sqrt{6\pi r^* W_{\text{ad}}F + (3\pi r^* W_{\text{ad}})^2}\right] \quad (8)$$

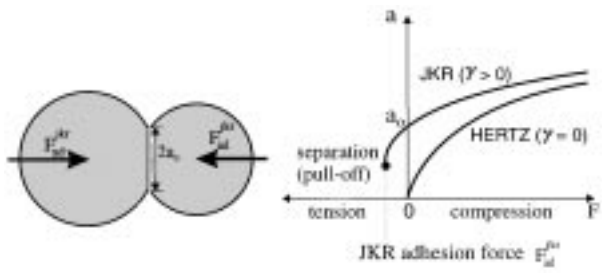

Fig. 1. Reversible contact-radius versus load curve of the nonadhesive (Hertzian) contact and adhesive (JKR) contact between two elastic spheres.

For reversible adhesion, the adhesion work is related to the surface and interfacial energies [see eqn (15)].

Without taking the surface energy into account, i.e. $W_{ad} = 0$, eqn (8) reverts to the simple Hertz equation[17,18]

$$a^3 = \frac{r^* F}{k_e^*} \cdot \tag{9}$$

At zero applied load, the contact radius a_o, is finite and given by

$$a_o^3 = \frac{6\pi W_{ad}(r^*)^2}{k_e^*} \cdot \tag{10}$$

Fig. 1 shows the differences of contact-radius versus load curve between the nonadhesive (Hertzian) contact and adhesive (JKR) contact under reversible thermodynamic conditions.

4 Derjaguin Approximation/Interaction Energy and Force

Generally, interaction energies rather than the forces experienced by molecules and particles have been dealt with in the literature. This is because most experimental data on molecular interactions are readily understood in terms of interaction energies. However, the forces between macroscopic bodies are often of greater interest, especially in our case for the DEM simulation, and are easier to measure than their interaction energies. In order to consider the adhesion effect in the DEM simulation, the adhesion energy W_{ad} in the eqn (8) has to be expressed in terms of interaction forces. Hereby, the Derjaguin approximation has been applied.

At very short surface distance h, i.e. r_1 and $r_2 \gg h$, the potential interaction force $F(h)$ between two spheres can be expressed by the so-called Derjaguin approximation:[3,19]

$$F(h)_{\text{sphere}} = 2\pi \frac{r_1 r_2}{r_1 + r_2} V(h)_{\text{plane}}, \tag{11}$$

where $V(h)_{\text{plane}}$ is the interaction energy per unit area of two planes at a surface distance h. Equation (11) is applicable to any type of force law, whether attractive, repulsive, or oscillatory, so long as the interaction range and the separation h is much less than the radii of the spheres.

If one sphere is very large, i.e. $r_2 \gg r_1$, the Derjaguin approximation corresponds to the limiting case of a sphere near a plane surface:

$$F(h)_{\text{sphere}} = 2\pi r V(h)_{\text{plane}} \tag{12}$$

In the case of two rigid (incompressible) spheres in contact ($h = \sigma_{hs}$), the interaction force or the adhesion force F_{ad} can be expressed by the adhesion work W_{132} if the interaction energy is regarded to be equal to the adhesion work, i.e. $V(\sigma_{hs}) = W_{132}$.[3] Hereby, $\sigma_{hs} \approx 0{\cdot}3$–$0{\cdot}6$ nm and is the hard spherical diameter of an atom or a molecule. For two spheres,

$$F_{ad} = 2\pi \frac{r_1 r_2}{r_1 + r_2} W_{132} \tag{13}$$

and for sphere/plane,

$$F_{ad} = 2\pi r W_{132} \tag{14}$$

can be applied. Equations (13) and (14) are a direct consequence of the Derjaguin approximation. W_{132} is the adhesion work and results from a contact process between two surfaces with material types 1 and 2 in a medium 3. In the case of reversible contact process, W_{132} can be determined by the following equation,[4,11]

$$W_{132} = \gamma_{12} - (\gamma_{13} + \gamma_{23}) \tag{15}$$

if the interfacial energies (γ_{13}, γ_{23} and γ_{12}) are known.

5 Application of Johnson–Kendall–Roberts (JKR) Theory

Equations (13) and (14) are valid for the rigid incompressible solid bodies. Real particles, however, are never completely rigid. They deform elastically if they come into contact under the influence of the attractive intersurface forces. These attractive forces can pull two spheres together and give rise to a finite contact radius a_o even under zero external load [see eqn (10)]. According to the JKR theory,[17] the nonlinear contact laws of Hertz[18] and of von Mindlin and Deresiewicz[20] have to be modified because of the intersurface adhesion. Another important result of the JKR theory predicts that on pulling two spheres from adhesive contact the contact radius decreases gradually from a_o to $0{\cdot}63a_o$ at which point the spheres spontaneously separate. The predicted adhesion force, or *pull-off* force, is 75% of that given by eqn (11) for undeformable rigid spheres, and can be shown as following: for two spheres,

$$F_{\mathrm{ad}}^{jkr} = \frac{3}{2}\pi\left(\frac{r_1 r_2}{r_1 + r_2}\right) W_{132} \tag{16}$$

and for sphere/plane,

$$F_{\mathrm{ad}}^{jkr} = \frac{3}{2}\pi r W_{132} \tag{17}$$

F_{ad}^{jkr} is independent of the original area of contact a_{o} and the elastic modulus of the spheres and can be regarded as the maximal attractive force between two elastic solid bodies without external load (see Fig. 1). This means that F_{ad}^{jkr} can be used as the lower limit of the total potential interaction force F_{p} in eqn (2). This lower force limit F_{ad}^{jkr} will not only determined by the van der Waals attraction part (F_{vdw}) but also by the electrostatic repulsion part (F_{el}), because the compact Stern or adsorbed layer changes the double-layer structure as well as the surface morphology. The change of surface morphology induces certainly the change of the interfacial energies and the change of adhesion work if the colloidal surfaces come into contact [see eqn (15)].

According to the relation $F_{\mathrm{ad}}^{jkr}(\sigma_{\mathrm{st}}) = F_{\mathrm{p}}(h)$, a shortest surface distanced (without external load) σ_{st} can be achieved, which is dependent of interfacial energies of contacting materials in liquid medium, form and size of the solid bodies [see eqns (2), (14) and (15)]. In the case of ceramic suspensions with electrolyte, this shortest intersurface distance will be determined mainly by the thickness of the compact Stern layer and will be much larger than the hard sphere diameter σ_{hs} for the case of solid bodies in vacuum.

The difficulties in the calculation of F_{ad}^{jkr} are due to the determination of adhesion work W_{132}. According to eqn (15), W_{132} is determined by the interfacial energies γ_{13}, γ_{23} and γ_{12}. In the case of solid bodies in suspensions,

$$W_{1L2} = \gamma_{12}^{L} - (\gamma_{1L} + \gamma_{2L}) \tag{18}$$

where the index L means liquid medium. For the same material type,

$$W_{1L1} = \gamma_{11}^{L} - 2\gamma_{1L}, \tag{19}$$

or

$$W_{SLS} = \gamma_{SS}^{L} - 2\gamma_{SL}, \tag{20}$$

where the index S means solid. The direct measurements of $\gamma_{1L}, \gamma_{2L}, \gamma_{SL}, \gamma_{12}^{L}, \gamma_{11}^{L}$, etc., in electrolyte suspensions are very difficult. The values of γ_{12}^{L} and γ_{11}^{L} in liquid medium are different from the values of γ_{12}^{V} and γ_{11}^{V} in vacuum ($\gamma_{11}^{V} = 0$ in vacuum), because the surface-morphological change resulted from the surface-chemical and/or -physical reactions with the liquid medium will not be completely eliminated through the solid-body contact. Therefore, the interaction forces are measured directly, and after that, F_{ad}^{jkr} are determined.[3,9,10,21–24] By using eqns (16) and (17), the adhesion work is calculated. And then by using eqn (18), the interfacial energies are obtained.[3,9,17,24]

6 Numerical Implementation and Physical Interpretation

According to the JKR theory [eqns (16) and (17)] and the formulation of the adhesion work in a contact process [eqns (18)–(20)], the JKR adhesion forces between two elastic solid bodies in liquid medium for the following cases can be derived and expressed through the interfacial energies:

1. Spheres with different materials and radii

$$F_{\mathrm{ad}}^{jkr} = \frac{3}{2}\pi\left(\frac{r_1 r_2}{r_1 + r_2}\right) \cdot W_{1L2} \quad \left(\text{Hereby, } W_{1L2} = \gamma_{12}^{L} - \gamma_{1L} - \gamma_{2L}\right) \tag{21}$$

2. Spheres with same material but different radii

$$F_{\mathrm{ad}}^{jkr} = \frac{3}{2}\pi\left(\frac{r_1 r_2}{r_1 + r_2}\right) \cdot W_{1L1} \quad \left(\text{Hereby, } W_{1L1} = \gamma_{11}^{L} - 2\gamma_{1L}\right) \tag{22}$$

3. Identical spheres

$$F_{\mathrm{ad}}^{jkr} = \frac{3}{4}\pi r \cdot W_{1L1} \quad \left(\text{Hereby, } W_{1L1} = \gamma_{11}^{L} - 2\gamma_{1L}\right) \tag{23}$$

4. Sphere on plane with different material

$$F_{\mathrm{ad}}^{jkr} = \frac{3}{2}\pi r \cdot W_{1L2} \quad \left(\text{Hereby, } W_{1L2} = \gamma_{12}^{L} - \gamma_{1L} - \gamma_{2L}\right) \tag{24}$$

Using the above-mentioned equations, the JKR adhesion forces F_{ad}^{jkr} can be calculated by the known adhesion work W or interfacial energies γ.

Through the application of the relation

$$F_{\mathrm{p}}(\sigma_{\mathrm{st}}) = F_{\mathrm{ad}}^{jkr} \tag{25}$$

and F_p from eqn (2), σ_{st} will be achieved. This lower limit of the potential forces F_{ad}^{jkr} is assumed to remain constant over the distance region for $0 < h < \sigma_{st}$. This assumption results to a linear potential function with a gradient of $m = -F_{ad}^{jkr}$. The potential at a surface distance h and inside this region can then be calculated by the following equation (see Fig. 2):

$$V(h) = V_{st} + F_{ad}^{jkr}(\sigma_{st} - h). \tag{26}$$

According to the Gouy–Chapman–Stern–Grahame model, such a linear dependence is a possible potential distribution inside the compact Stern layer between ceramic surfaces and aqueous electrolyte solution.[25,26] At a surface distance $h < \sigma_{st}$, the adhesion mechanics are valid (see Section 3). This distance σ_{st} is determined by the surface morphologies (or the adhesion work) of contacting bodies, corresponds to the thickness of Stern layer, and will not be overcome without external load.

Figure 3 shows the connections between the DLVO potential interaction, the JKR adhesion and the solid-body contact of two elastic spheres in an electrolyte suspension. In Fig. 3(a), the defined elastic contact radius a_o [see eqn (10)], the shortest surface distance without external load σ_{st} [see eqn (25)] and the relative displacement of both spherical centers $\Delta\delta$ are shown. σ_{st} and a_o result merely from the JKR adhesion force (F_{ad}^{jkr}) or the adhesion work (W) without external load. This fictitious overlap of both spheres $\Delta\delta$ depends on the flattening of both spheres. This flattening can be given rise to adhesion and/or external load. In Fig. 3(b), the potential and force curves versus the surface

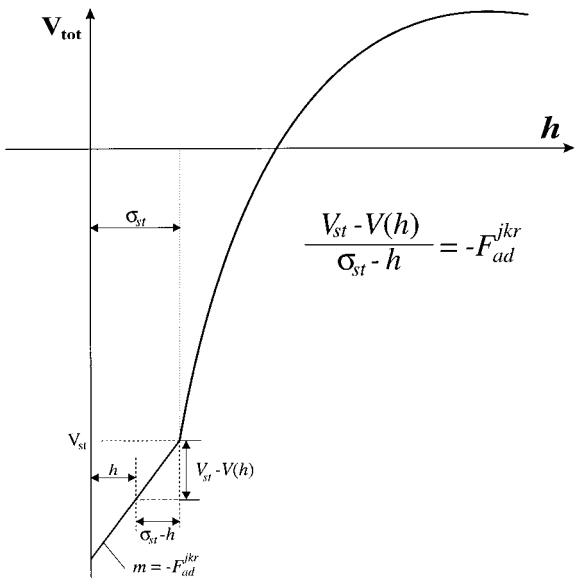

Fig. 2. Calculation of the potential function inside the distance region of $h < \sigma_{st}$.

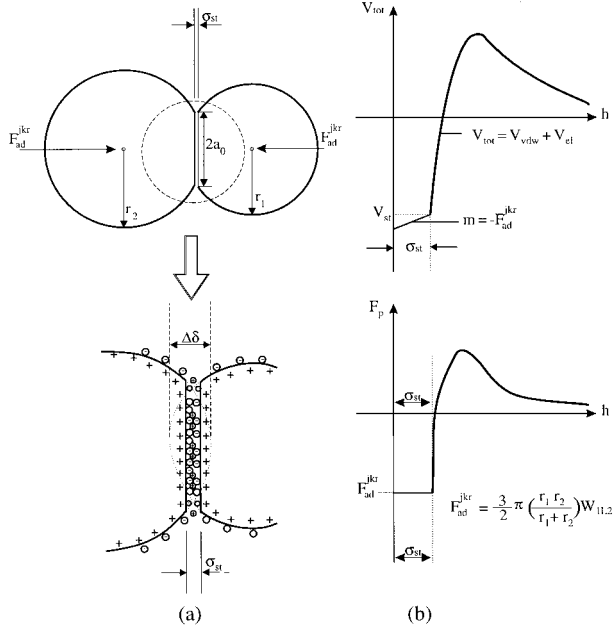

Fig. 3. Schematic presentation of the physical connections between the DLVO potential interaction, the JKR adhesion and the solid-body contact of two elastic spheres in an electrolyte suspension.

distance h are shown. Hereby, F_p is the negative differentiation of V_{tot} at h [see eqn (2)], which is also valid in the distance region of $h < \sigma_{st}$. Figure 4 shows the physical connections between the van der Waals attraction, the JKR adhesion and the solid-body contact between a sphere and a plane wall in an electrolyte suspension. In this case, no electrostatic double layer on the plane wall is assumed.

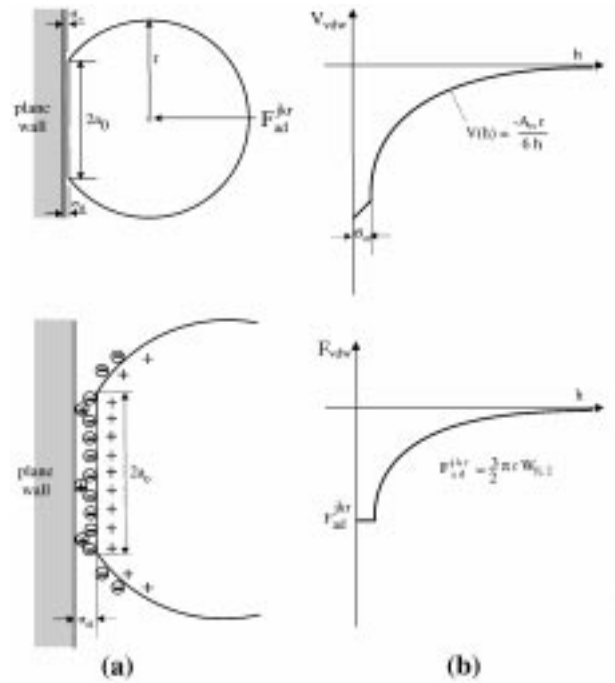

Fig. 4. Schematic presentation of the physical connections between the van der Waals attraction, the JKR adhesion and the solid-body contact between a sphere and a plane wall in an electrolyte suspension. No electrostatic double layer on the plane wall is assumed.

7 DEM Simulation

The above-mentioned formulations, especially eqns (1)–(10) and eqns (21)–(25), have been implemented into the simulation program *DemCop* based on the DEM. The program name *DemCop* is the abbreviation for 'Discrete Element Modelling of Colloidal Powder Processing' and was developed recently.[2,6–8] Besides the above-described DLVO long-range interactions (V_{vdw} and V_{el}), adhesion, elastic solid-body contacts JKR theory, etc., the medium influences, e.g. frictional drag, rotational resistance, hydrodynamic lift, gravitation force and hydrostatic lift were taken into account for simulation.[8] Meanwhile, it was found that the Brownian force is important only for particles with diameter less than 100 nm.[8] Therefore, the Brownian force was omitted in the following simulations. This DEM simulation method regards each particle as an individual element. The response of each element to mechanical and electrical impact from its surroundings can be described by the summation of all interactions, e.g. particle–particle, particle–medium, particle–boundary, and particle–external force field interaction. Thus, this method can be used to study the particle packing dynamics during colloidal forming processes. There are not only the fundamental questions concerning materials science like deflocculation, agglomeration, pore and chain formation, phase/size separation, defect formation, etc. can be analysed, but also the knowledge for improving the ceramic forming techniques using colloidal suspensions (also multiphase) can be achieved.

In order to show the transition effects from the long-range potential interaction to the solid-body contact in the consolidation processes, two-phase suspensions made of 200 Al_2O_3 and 200 ZrO_2 particles (tri-modal, $d = 0{\cdot}55$, $0{\cdot}45$ and $0{\cdot}35\,\mu$m) in a square box of $25{\cdot}47 \times 12{\cdot}74\,\mu$m are centrifuged under a centrifugal acceleration of $3000g$ to the right and the gravitation g downwards (see Fig. 6). This corresponds to an area density of $\rho_A = 20\%$. Hereby, the particles and the interaction models are three-dimensional, but the particle movement is restricted on a two-dimensional plane. The densities are $\rho_{Al_2O_3} = 3{\cdot}8\,g\,cm^{-3}$ und $\rho_{ZrO_2} = 5{\cdot}8\,g\,cm^{-3}$. The Zeta potential curves versus pH values of Al_2O_3 (A) and ZrO_2 (Z) have almost the same dependence, where the Al_2O_3 curve lies with a small amount higher than the ZrO_2 curve.[27] Therefore, $\zeta Al_2O_3 = 50\,mV$ and $\zeta ZrO_2 = 40\,mV$ are assumed for the stabilized two-phase suspensions. The Hamaker constants of Al_2O_3–Al_2O_3 (A–A) and ZrO_2–ZrO_2 (Z–Z) are assumed to be A_H (A–A) $= 5{\cdot}2 \times 10^{-20}$ J and A_H (Z–Z) $8{\cdot}8 \times 10^{-20}$ J, respectively.[28] The Hamaker constant between Al_2O_3 and ZrO_2 is unknown and is assumed to have a smaller value of $A_H(A-Z) = 2{\cdot}0 \times 10^{-20}$ J, so that the different phases will have a smaller attractive force. Likewise, the adhesion work between Al_2O_3 and ZrO_2 is assumed to have a smaller value than Al_2O_3–Al_2O_3 and ZrO_2–ZrO_2, namely $W_{ad}(A-Z) = -1\,mJ\,m^{-2}$ and $W_{ad}(A-A) = W_{ad}(Z-Z) = -3\,mJ\,m^{-2}$. The suspensions are assumed to have a lower ionic strength with a Debye–Hückel parameter of $\kappa = 10^7\,m^{-1}$.

Using the above-mentioned parameters and the DLVO potential interaction functions in Section 2, the potential interaction force F_p curves versus the interparticle surface distance h for the stabilized suspension systems are shown in Fig. 5(a). The inset figure shows the dependences inside the short surface distance region of $h < 1{\cdot}5$ nm. Hereby, $\sigma_{st}(Z-Z) = 1{\cdot}0$ nm, $F_{ad}^{jkr}(Z-Z) = -1{\cdot}6 \times 10^{-9}$ N, $\sigma_{st}(A-A) = 0{\cdot}7$ nm, $F_{ad}^{jkr}(Z-Z) = -1{\cdot}95 \times 10^{-9}$ N, $\sigma_{st}(A-Z) = 0{\cdot}35$ nm and $F_{ad}^{jkr}(A-Z) = -2{\cdot}3 \times 10^{-9}$ N can be found. The initial state before casting is shown in Fig. 6(a). After a casting time of $t = 5{\cdot}25$ ms, chain formation near

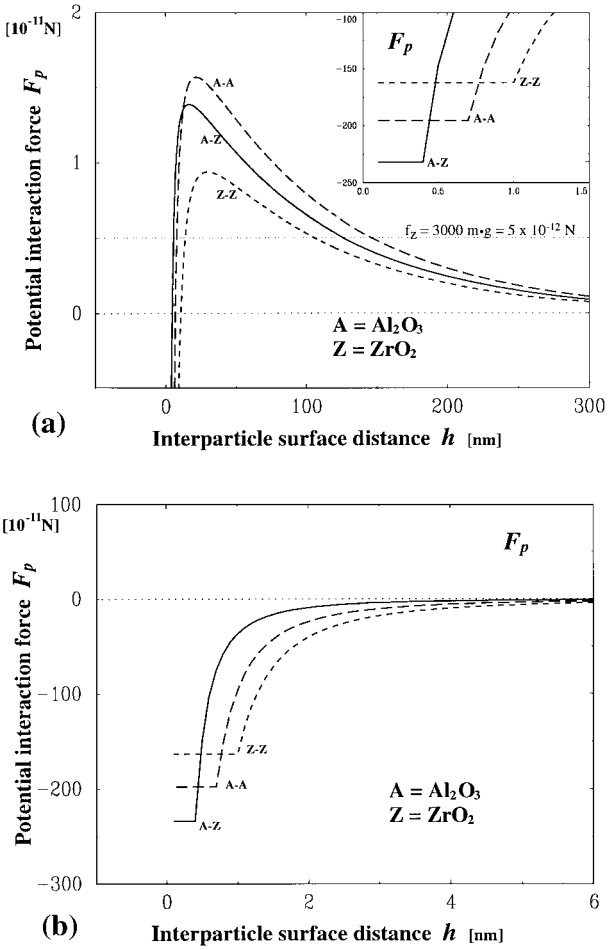

Fig. 5. The potential interaction force curves versus the interparticle surface distance: (a) in the stabilized suspensions with $\zeta_{Al_2O_3} = 50\,mV$, $\zeta_{ZrO_2} = 40\,mV$; (b) in the flocculated suspensions with $\zeta_{Al_2O_3} = \zeta_{ZrO_2} = 0\,mV$. $\kappa = 10^7\,m^{-1}$ and $d_{Al_2O_3} = d_{ZrO_2} = 0{\cdot}45\,\mu$m are assumed for both cases.

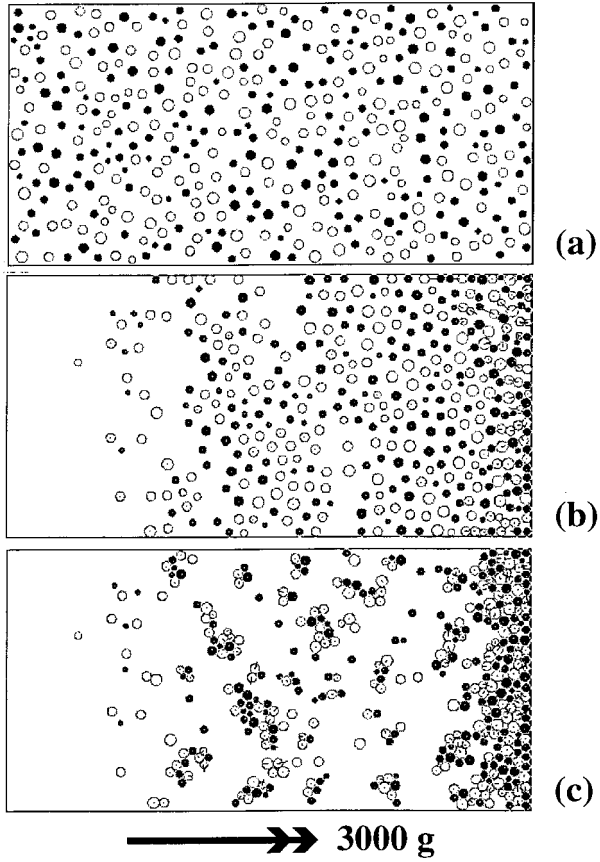

Fig. 6. Intermediate states of the DEM simulations during centrifugal casting of Al_2O_3 (bright)/ZrO_2 (dark) suspensions with a centrifugal acceleration of 3000 g after a casting time of $t = 5{\cdot}25$ ms: (a) initial state; (b) stabilized suspension [corresponds to Fig. 5(a)]; (c) flocculated suspension [corresponds to Fig. 5(b)]. The dash lines on particles are the velocity vectors of particles.

the bottom of sediment has been observed [see Fig. 6(b)]. The particles reach the bottom and pile up successively, so that the summation of all centrifugal forces on each pile-up-particles can overcome the maximal repulsive force (barrier) between two electrostatic stabilized particles. Thus, the particles will adhere to each other and build up chains from the bottom. The chains will grow up if the casting process continues. Schematically, the centrifugal force of a ZrO_2 particle with $d = 0{\cdot}45$ μm amounts to

$$f_z = 3000 \text{ m} \times g \approx 5 \times 10^{-12} \text{ N}$$

which is 1/2–1/3 of the maximal repulsive forces [see Fig. 5(a)]. This means that the particles on the bottom will adhere to each other and build up chains if there are more than three pile-up-particles. Away from the bottom of sediment, the repulsive force dominates between the particles, therefore there is no formation to be observed.

In the case of flocculated suspensions, i.e. $\zeta_{Al_2O_3} = \zeta_{ZrO_2} = 0$ mV, a different packing structure can be observed [Fig. 6(c)]. F_p curves versus h are shown in Fig. 5(b). No electrostatic repulsive forces between the particles are assumed, therefore the particles agglomerate before they have sedimented upon the bottom. Each of the small agglomerates behave like big particles and sediment much faster than the stabilized (or isolated) particles. Thus, after a same casting time, there are more particles in the flocculated suspensions have been sedimented than in the stabilized suspensions. An analysis of the mechanisms for chain formation and agglomeration was given elsewhere.[7]

8 Conclusions

In this work, the Derjaguin approximation and the JKR theory have been successfully applied to solve the transition problems from the DLVO long-range interaction to the elastic solid-body contact for the numerical simulations based on the discrete element method (DEM). Meanwhile, this work emphasizes the mathematical modelling and its numerical realization of the singularity problem by using the explicit interaction functions derived from the continuum assumptions. Hereby, the adhesion work (or energy) is assumed to be identical with the DLVO interaction energy at a shortest reachable surface distance without external load (i.e. at the primary minimum), and the JKR adhesion force is assumed to be equivalent to the lower limit of the DLVO interaction force. Besides, the shortest surface distance without external load approximates the thickness of Stern layer and is dependent on the surface morphology described by the interfacial energy or the adhesion work during the surfaces in contact.

These physical models or assumptions describe reasonable physical reality in the colloid science. For example, two surfaces in aqueous solution with higher electrolyte concentration result in a lower adhesion work due to the higher covering rate of the activer colloid surface through the electrolytic ions in solution, a lower JKR adhesion force and a thicker Stern layer or a longer shortest surface distance without external load if they come into contact. Within the Stern layer, the adhesion force is assumed to be constant and induces the elastic deformation, and according to eqn (2), the interaction potential varies linearly. This assumption of the linear dependence of the potential interaction inside the Stern layer is certainly a simplification. However, it is a good assumption for studying the particle packing behaviour of submicron powders, because the thickness of the Stern layer usually amounts to less than 1·5 nm which is much smaller than the size of the

considered particles with $d > 300$ nm, and thus the resulted packing structures will not be decisively determined by the interactions inside this region, but by the DLVO long-range interaction and the adhesion. For the case of nanosized particles, the interaction functions inside the Stern layer will become important for the formation of the packing structures.

The assumptions and formulations in this work give us not only solutions for the numerical sigularity problems between the DLVO long-range interaction functions and the JKR theory for the elastic solid-body contact but also reasonable physical interpretations. Furthermore, the results of DEM simulation based on these assumptions and formulations have shown this transition phenomena correctly.

References

1. Kendall, K., Alford, McN. N., Clegg, W. J. and Birchall, J. D., High strength and weibull modulus from colloidal processing of ceramics. *Brit. Ceram. Proc.*, 1990, **45**, 79–89.
2. Hong, C.-W. and Greil, P., Discrete element modelling of colloidal powder processing, *Ceramic Transactions*, Vol. 54 *Science, Technology, and Applications of Colloidal Suspensions*. American Ceramic Society, Columbus, OH, 1995, pp. 235–249.
3. Israelachvili, J. N., *Intermolecular and Surface Forces*, 2nd edn. Academic Press, London, 1985.
4. Hiemenz, P. C., *Principles of Colloid and Surface Chemistry*. Marcel Dekker, New York, 1986.
5. Lyklema, J., The colloidal background of agglomeration. In *4th International Symposium on Agglomeration*, Toronto, Canada, 2–5 June 1985, ed. C. E. Capes, L. G. Kuhn, Ottowa, pp. 23–36.
6. Hong, C.-W., Computer-aided process modelling of colloidal powder forming. *Fortschrittsbericht der DKG*, 1995, **10**(4), 225–241 (in German).
7. Hong, C.-W., Discrete element modelling of colloidal packing dynamics during centrifugal casting. *J. Ceram. Soc. Jpn.*, 1996, **104**(9), 793–795.
8. Hong, C. W., New concept for simulating particle packing in colloidal forming processes. *J. Am. Ceram. Soc.*, 1997, **80**(10), 2517–2524.
9. Israelachvili, J. N., Adhesion forces between surfaces in liquids and condensable vapours. *Surf. Sci. Rep.*, 1997, **14**, 109–159.
10. Pashley, R. M. Hydration forces between mica surfaces in aqueous electrolyte solutions. *J. Colloid Interface Sci.*, 1981, **80**(1), 153–162.
11. Hunter, R. J., *Foundations of Colloid Science*, Vol. 1. Clarendon Press, Oxford, 1992.
12. Mahanty, J., and Ninham, B. W., *Dispersion Forces*. Academic Press, London, 1976.
13. Russel, W. B., *The Dynamics of Colloidal Systems*. The University of Wisconsin Press, Madison/Wisconsin, 1987.
14. Bell, G. M., Levine, S. and McCartney, L. N., Approximate methods of determining the double-layer free energy of interaction between two charged colloidal spheres. *J. Colloid Interface Sci.*, 1970, **33**(3), 335–359.
15. Ives, K. J. and Gregory, J., Surface forces in filtration. (Proceedings of the Society for Water Treatment and Examination, 1966, **15**, 93–116.
16. Hunter, R. J., *Foundations of Colloid Science*, Vol. II. Clarendon Press, Oxford, 1991.
17. Johnson, K. L., Kendall, K. and Roberts, A. D., Surface energy and the contact of elastic solids. *Proc. R. Soc. Lond. A.*, 1971, **324**, 301–313.
18. Johnson, K. L., *Contact Mechanics*. Cambridge University Press, Cambridge, 1985.
19. Derjaguin, B. V., Untersuchungen über die Reibung und Adhäsion, IV: Theorie des Anhaftens kleiner Teilchen. *Kolloid Zeitschrift*, 1934, **69**(2), 155–164.
20. Mindlin, R. D. and Deresiewicz, H., Elastic spheres in contact under varying oblique forces. *J. Appl. Mech.*, 1953, **20**, 327–344.
21. Israelachvili, J. N. and Adams, G. E., Measurement of forces between two mica surfaces in aqueous electrolyte solutions in the range 0–100 nm. *J. Chem. Soc. Faraday Trans.*, 1978, **74**, 975–1001.
22. Pashley, R. M., DLVO and hydration forces between mica surfaces in Li_+, Na_+, K_+, and Cs_+ electrolyte solutions: a correlation of double-layer and hydration forces with surface cation exchange properties. *J. Colloid Interface Sci.*, 1981, **83**(2), 531–546.
23. Horn, R. G., Smith, D. T. and Haller, W., Surface forces and viscosity of water measured between silica sheets. *Chem. Phys. Lett.*, 1989, **162**, 404–408.
24. Horn, R. G., Surface forces and their action in ceramic materials. *J. Am. Ceram. Soc.*, 1990, **73**(5), 1117–1135.
25. Hunter, R. J., *Zeta Potential in Colloid Science*. Academic Press, London, 1981.
26. James, R. O., Characterization of Colloids in Aqueous Systems, *Advances in Ceramics, Vol. 21 Ceramic Powder Science*. The American Ceramic Society, Columbus, OH, 1987.
27. Bleier, A., Acid-base properties of ceramic powders. In *Materials Science Research, Vol. 15, Advances in Materials Characterization*, ed. D. R. Rossington, R. A. Condrate and R. L. Snyder. Plenum Press, New York, 1983.
28. Bergström, L., Meurk, A., Arwin, H. and Rowcliffe, D. J., Estimation of Hamaker constants of ceramic materials from optical data using Lifshitz theory. *J. Am. Ceram. Soc.*, 1996, **79**(2), 1339–1348.